Available online at www.sciencedirect.com
SCIENCE DIRECT®
Biochemical and Biophysical Research Communications 337 (2005) 232–240
BBRC
www.elsevier.com/locate/ybbrc

Proteolytic processing of the ovine prion protein in cell cultures

Heidi Tveit [a], Christoffer Lund [b], Christel M. Olsen [b], Cecilie Ersdal [b,c], Kristian Prydz [a], Ingrid Harbitz [b], Michael A. Tranulis [b,*]

[a] Department of Molecular Biosciences, University of Oslo, P.O. Box 1041 Blindern, N-0316 Oslo, Norway
[b] Department of Basic Sciences and Aquatic Medicine, Norwegian School of Veterinary Science, P.O. Box 8146 Dep., N-0033 Oslo, Norway
[c] Department of Production Animal Clinical Sciences, Norwegian School of Veterinary Science, P.O. Box 8146 Dep., N-0033 Oslo, Norway

Received 30 August 2005
Available online 15 September 2005

Abstract

The cellular compartment and purpose of the proteolytic processing of the prion protein (PrP) are still under debate. We have studied ovine PrP constructs expressed in four cell lines; murine neuroblastoma cells (N2a), human neuroblastoma cells (SH-SY5Y), dog kidney epithelial cells (MDCK), and human furin-deficient colon cancer cells (LoVo). Cleavage of PrP in LoVo cells indicates that the processing is furin independent. Neither is it reduced by some inhibitors of lysosomal proteinases, proteasomes or zinc-metalloproteinases, but incubation with bafilomycin A_1, an inhibitor of vacuolar H^+/ATPases, increases the amount of uncleaved PrP in the apical medium of MDCK cells. Mutations affecting the putative cleavage site near amino acid 113 reveal that the cleavage is independent of primary structure at this site. Absence of glycosylphosphatidylinositol anchor and glycan modifications does not influence the proteolytic processing of PrP. Our data indicate that PrP is cleaved during transit to the cell membrane.

Keywords: Prion protein; Proteolytic processing; Cell culture; Ovine

A key molecular event in prion diseases, such as Creutzfeldt–Jakob disease in human and scrapie in sheep, is the poorly understood conversion of normal cellular glycosylphosphatidylinositol (GPI)-anchored prion protein (PrP^C, herein referred to as PrP) into a malformed and dysfunctional conformer (PrP^{Sc}) that is partly proteinase resistant, reviewed in [1]. In normal brain and several other tissues, as well as in cultured cells, PrP is to varying degrees proteolytically processed near amino-acid 113 (numbering according to ovine PrP), N-terminal to a hydrophobic region of the protein [2–5]. This highly consistent proteolytic processing of PrP separates the structurally disordered Cu^{2+}-binding domain of the protein from the globular C-terminal two-thirds. The precise cellular site of this cleavage and its possible role for the cellular function of PrP are still a matter of controversy. Concerning the cellular compartment for the cleavage, however, the consensus appears to be that PrP is processed during cycling between the plasma membrane and endosomes, and that there are at least two possible cleavage sites within the N-terminal portion of PrP [3–6]. For a detailed analysis of the heterogeneity of brain PrP, see [7]. The major cleavage, which is the focus of this work, has been shown to destroy the epitope for the monoclonal antibody 3F4 [5]. This epitope is naturally present in human and hamster PrP, and has an absolute requirement for the sequence MKHM (109–112) immediately N-terminal to the hydrophobic stretch of PrP [8]. Sequence analysis of fragmented PrP derived from human neuroblastoma cells has indicated that the major cleavage site resides in the C-terminal portion of the 3F4 epitope [5], which corresponds to amino-acids 112–115 in the ovine PrP. Cleavage of hamster PrP expressed in N2a cells was shown to be insensitive to neutralisation of acidic compartments by NH_4Cl treatment, suggesting that this is an event distinct from the general breakdown of PrP in lysosomes [9]. However, studies of chicken PrP expressed in N2a cells indicated that inhibition of lysosomal

* Corresponding author. Fax: +47 22 59 73 10.
E-mail address: Michael.Tranulis@veths.no (M.A. Tranulis).

0006-291X/$ - see front matter © 2005 Elsevier Inc. All rights reserved.
doi:10.1016/j.bbrc.2005.09.031

proteases by various agents, including NH_4Cl, reduced the liberation of N-terminal cleavage products into the culture medium [4]. Since GPI-anchored proteins appear to cluster into dynamic microdomains, rafts, of the lipid bi-layer, it has been suggested that the cleavage of PrP could be performed by proteinases specifically localised to such membrane domains [9]. More recently, it has been suggested that the fibrinolytic serine proteinase plasmin can be involved in the cleavage of PrP [10,11].

The general breakdown of PrP in crude human brain homogenate was strongly inhibited by metal chelators such as EDTA and EGTA, an effect that could be directly reversed by addition of Fe^{2+} and Cu^{2+} ions. Other classes of proteinase inhibitors had minor effects on the breakdown of PrP [12]. Interestingly, inhibition of the disintegrins ADAM10 (a disintegrin and metalloproteinase) and TACE (tumor necrosis factor α converting enzyme, ADAM17) reduced the liberation of the N-terminal portion of PrP to the cell culture medium of human embryonic kidney cells [13], pointing to a possible role for these zinc metalloproteinases in the proteolytic processing of PrP. Another study found that an α-secretase like activity, possibly raft-associated, can be involved in phorbol ester-stimulated shedding of full-length PrP by cleaving the extreme C-terminus of the PrP [14].

Most studies of the proteolytic processing of PrP in cell culture have focused on C-terminal PrP fragments in cell lysates and N-terminal fragments in conditioned media. The fate of the N-terminal tail has proven difficult to study, not least due to its size, which is somewhere between 7 and 9 kDa. To circumvent this problem we have generated several PrP constructs carrying green fluorescent protein (GFP) within the N-terminal portion of the protein. Similar PrP::GFP chimaeras have been used by a number of other groups [15–18]. In general, the cellular processing and behaviour of PrP when fused with GFP in this way appear normal. Herein, we compare the proteolytic processing of PrP::GFP fusion proteins in different cell lines and in the presence of different proteinase inhibitors. Our data indicate that the processing of PrP::GFP fusion proteins occurs according to the same pattern as for un-tagged PrP. Furthermore, this processing appears insensitive to mutations affecting the proposed major cleavage site and is independent of GPI anchoring and glycan modifications of the protein. However, treatment with bafilomycin A_1 (Baf A_1), an inhibitor of vacuolar H^+/ATPases, allowed more uncleaved PrP to be detected, particularly in the apical medium of MDCK cells. Interestingly, the processing of amyloid precursor protein (APP) by β-secretase (BACE 1), which is of major importance in Alzheimer's disease, is also reduced by Baf A_1 [19]. Our data suggest that PrP is constitutively processed, possibly in a slightly acidic compartment during transit through the secretory pathway, en route to the plasma membrane.

Materials and methods

Sheep brain tissue

Crude preparations of PrP-rich microsomal and synaptosomal membranes from sheep brain were produced as described [20]. Briefly, immediately after euthanasia with pentobarbital and exsanguination through the carotid arteries, 40 g of brain tissue was homogenised in 200 ml ice-cold buffer containing 0.32 M sucrose, 0.5 mM KCl, 1 mM Mg_2Cl, 1 mM $NaHCO_3$, 1 mM EDTA supplemented with proteinase inhibitor tablets (Complete, Roche), and 1 mM dithiothreitol (DTE). The homogenate was centrifuged at 3000*g* for 10 min at 4 °C. The pellets were rehomogenised in 170 ml of the same buffer and centrifuged at 3000*g* for 10 min at 4 °C. Supernatants were centrifuged through a 0.85 M sucrose cushion at 100,000*g* for 1 h at 4 °C. The pellets were resuspended in lysis buffer (LB) containing 50 mM Tris–HCl (pH 7.4), 150 mM NaCl, 0.5% (v/v) Triton X-100, 0.5% sodium deoxycholate, and 1 mM EDTA, supplemented with Complete proteinase inhibitor tablets (Roche).

DNA constructs

The primers used in cloning of the PrP constructs are shown in Table 1.

PrP-pGEM T-Easy. The ovine prion protein was initially cloned into the pGEM-T Easy vector (Promega) using the Expand Long Template PCR System (Roche), primer 1 and 2, and genomic DNA as template.

PrP-pcDNA3. The coding region of PrP was amplified from PrP-pGEM T-easy using primer 3 and 4 containing an *Eco*RI and a *Xho*I restriction site, respectively, and cloned into pGEM-T Easy. PrP was cut out with the restriction enzymes *Eco*RI and *Xho*I, and ligated into the corresponding restriction sites of the expression vector pcDNA3 (Invitrogen).

PrP::GFP-pcDNA3. A GFP-labelled PrP was constructed by ligating GFP into the *Xma*I site of PrP-pGEM-T Easy. GFP was amplified from pEGFP-C1 (Clontech) using primer 5 and 6 containing *Xma*I sites, and cloned into pGEM-T Easy. After *Xma*I digestion of the plasmid, GFP was ligated into *Xma*I digested PrP-pGEM-T Easy. The restriction enzymes *Eco*RI and *Xho*I were used to transfer the PrP-GFP from pGEM T-Easy to pcDNA3.

PrP::GFPΔGPI-pcDNA3. A secretory PrP::GFP was constructed by introducing a stop codon at the GPI-anchoring site (Ser234Stop) using PrP::GFP-pcDNA3 as template, and primer 7 and 8 containing an *Eco*RI and a *Xho*I restriction site, respectively. The amplification product was cloned into pGEM-T Easy. PrP::GFPΔGPI was cut out with *Eco*RI and *Xho*I, and ligated into pcDNA3.

All DNA constructs were sequenced to confirm correct amplification and cloning.

Site-directed mutagenesis

Mutations were generated by PCR-mediated mutagenesis in PrP::GFP-pcDNA3 using QuickChange II Site-directed Mutagenesis Kit (Stratagene). Mutation V115M introduced the human and hamster epitope 3F4 into the ovine PrP::GFP. The forward (F) and reverse (R) primers used in the site-directed mutagenesis are shown in Table 1. All mutations were verified by sequencing.

Cell cultures

Madin–Darby canine kidney (MDCK II) cells were grown in DMEM (Dulbecco's modified Eagle's medium, Cambrex) with addition of 1% glutamine (Cambrex) and 5% foetal bovine serum (FBS, PAA, Australia). The neuroblastoma cell lines N2a (murine) and SH-SY5Y (human) were kindly provided by Dr. Jörg Tatzelt (Max Planck Institute of München, Germany). N2a cells were grown in minimum essential medium (MEM, Sigma) added 10% FBS (Euroclone), non-essential amino-acids, and pyruvate (Cambrex). SH-SY5Y were grown in DMEM with 10% FBS (Euroclone). Human furin-deficient colon cancer cells (LoVo) transfected

Table 1
Listing of primers used in this study

1	PrP-pGEM T-easy F	5′-CACCCTCTTTATTTTGCAGAGAAGT-3′
2	PrP-pGEM T-easy R	5′-AAGATAATGAAAACAGGAAGGTTGC-3′
3	PrP-pcDNA3 F	5′-ATCG**GAATTC**TATGGTGAAAAGCCACATAG-3′
4	PrP-pcDNA3 R	5′-ATTAG**CTCGAG**TACTATCCTACTATGAGAAAAAT-3′
5	PrP::GFP-pcDNA3 F	5′-GCTTAATTAGT**CCCGGG**AATGGTGAGCAAGGGCGAGGA-3′
6	PrP::GFP-pcDNA3 R	5′-ATTAGTACTAT**CCCGGG**TACTTGTACAGCTCGTCCAT-3′
7	PrP::GFPΔGPI-pcDNA3 F	5′-ATCG**GAATTC**TATGGTGAAAAGCCACATAG-3′
8	PrP::GFPΔGPI-pcDNA3 R	5′-ATTAG**CTCGAG**TACTATGCCCCCCTTTGGTAATAA-3′
9	K113R F	5′-GCCAAAAACCAACATG***AGG***CATGTGGCAGGAGCTGCTGC-3′
10	K113R R	5′-GCAGCAGCTCCTGCCACATG***CCT***CATGTTGGTTTTTGGC-3′
11	K1113A F	5′-GCCAAAAACCAACATG***GCC***CATGTGGCAGGAGCTGCTGC-3′
12	K1113A R	5′-GCAGCAGCTCCTGCCACATG***GGC***CATGTTGGTTTTTGGC-3′
13	KHV113-115AAA F	5′-GCCAAAAACCAACATG***GCCGCCGCC***GCAGGAGCTGCTGC-3′
14	KHV113-115AAA R	5′-GCAGCAGCTCCTGC***GGCGGCGGC***CATGTTGGTTTTTGGC-3′
15	K113D F	5′-GCCAAAAACCAACATG***GAC***CATGTGGCAGGAGCTGCTGC-3′
16	K113D R	5′-GCAGCAGCTCCTGCCACATG***GTC***CATGTTGGTTTTTGGC-3′
17	V115M F	5′-GCCAAAAACCAACATGAAGCAT***ATG***GCAGGAGCTGCTGC-3′
18	V115M R	5′-GCAGCAGCTCCTGC***CAT***ATGCTTCATGTTGGTTTTTGGC-3′

Forward (F) and reverse (R) primers used in the construction of PrP-expression plasmids (1–8) and in site-directed mutagenesis (9–18). Restriction sites are indicated in bold. Codons specifying mutated amino acids are presented in bold and italics.

with the murine furin gene (LoVo/LF36) and with control vector (LoVo/neo) were indirectly provided by Dr. E. Mekada (Kurume University, Kurume, Japan). LoVo cells were grown in F-12 media (Cambrex) added 10% FBS (Euroclone). All cells were grown at 37 °C and 5% CO_2 with 1% penicillin/streptomycin.

In order to study the sorting of PrP in polarised epithelial cells, MDCK II cells transfected with PrP::GFP or PrP::GFPΔGPI were grown for 3 days on 4.7 cm^2 polycarbonate filters (Costar 3412), to establish confluent monolayers, before incubation for 16 h in serum-free medium. The apical and basolateral media and cell fractions were then harvested.

Transfection and drug treatment

MDCK II cells were transfected with FUGENE 6 (Roche). Lipofectamine and Plus reagents (Invitrogen) were used to transfect the other cell lines according to the manufacturer's instructions. Stably transfected cells were selected with G-418-sulphate (Duchefa, NL and PAA Laboratories) at a concentration of 0.5 mg/ml (SH-SY5Y) and 1 mg/ml (MDCK II and N2a). For the N2a cells the concentration was gradually reduced to 0.35 mg/ml after some weeks. Several colonies were initially selected from each cell line. After screening for fluorescence intensity (Olympus IX81 fluorescence microscope) and PrP signals on Western blots, one clone was selected from each cell line for further studies. Transiently transfected cells were harvested 24 h after transfection.

Exposure of cells to drugs was performed in OPTI-MEM (Gibco-BRL Life Technologies) for different time intervals as indicated in the figure legends. The cells were exposed to the following chemicals; leupeptin, NH_4Cl, and galardin from Sigma–Aldrich, aprotinin (Roche), lactacystin (Calbiochem), and Baf A_1 (a gift from Astra Zeneca). Cells grown on filters were exposed to the same concentration of drugs in apical and basolateral media. After collection of conditioned media, cells were lysed in LB for 1 h on ice.

Antibodies

The monoclonal antibodies (MAbs) SAF32 (Cayman), P4 and L42 (Food Diagnostics), 6H4 and 34C9 (Prionics), and 3F4 (Sigma–Aldrich) were used in this study. Figs. 1A and 2A show a schematic representation of the binding sites to PrP. In Western blots, primary antibodies were used in 0.05–0.2 μg/ml concentrations. Secondary antibodies, goat-anti-mouse, conjugated with horseradish peroxidase (HRP, Bio-Rad and Molecular Probes), alkaline phosphatase (ALP, Molecular Probes) or Alexa-594 (Molecular Probes) were used in 0.05–0.3 μg/ml concentrations for detection with enhanced chemiluminescence (HRP) or fluorescence (ALP and Alexa-594).

Enzymatic deglycosylation, Western blot, and quantification analysis

Post-nuclear supernatants were produced by centrifugation of cell lysates for 5 min at 1000*g*. Conditioned culture media were analysed without prior concentration of proteins. For enzymatic deglycosylation samples were treated with *N*-glycosidase F (PNGase F, New England Biolabs) for 1 h at 37 °C, as recommended by the manufacturer. Prior to electrophoresis, proteins were boiled for 5 min in SDS sample buffer (NuPAGE, Invitrogen) in the presence of a reducing agent (Invitrogen). Proteins were separated by electrophoresis on precast 12% Bis-Tris polacrylamide gels (XT-Criterion, Bio-Rad), with XT-MOPS (Bio-Rad) as the running buffer. The proteins were electro-blotted at 25 V for 45 min with Tris/CAPS transfer buffer as recommended by the supplier (Trans Blot Semi-Dry, Bio-Rad) onto polyvinylidene difluoride membranes (Hybond-P, Amersham Biosciences). To reduce unspecific binding of antibodies, membranes were blocked by incubation with 5% (w/v) fat-free dried milk (Bio-Rad) in TBS for 1 h at room temperature (RT). Incubations with antibodies were performed in TBS with 0.1% Tween 20 and 1% (w/v) fat-free dried milk overnight at 4 °C for primary antibodies and for 1 h at RT for secondary antibodies. Visualisation of bands was achieved with enhanced chemiluminescence (ECL Plus, Amersham Biosciences), captured by ECL Hyperfilm (Amersham Biosciences) or by fluorescence scanning with a variable mode imager (Typhoon 9200, Amersham Biosciences) when secondary antibodies labelled with ALP or fluorochromes were used. The Image Quant software (Amersham Biosciences) was used for quantitative analysis of bands.

Results

We have conducted comparative studies of the proteolytic processing of PrP in various cell lines by taking advantage of GFP as a protein marker. Ovine PrP and different PrP::GFP fusion proteins are illustrated in Fig. 1A. The N-terminal PrP fragment, which in native PrP is 7–9 kDa, appears with a molecular mass of approximately 36 kDa in the PrP::GFP fusion protein. See Table 2 for an overview of molecular masses of PrP and PrP::GFP proteins and fragments. As evident from Fig. 1B, PrP::GFP is

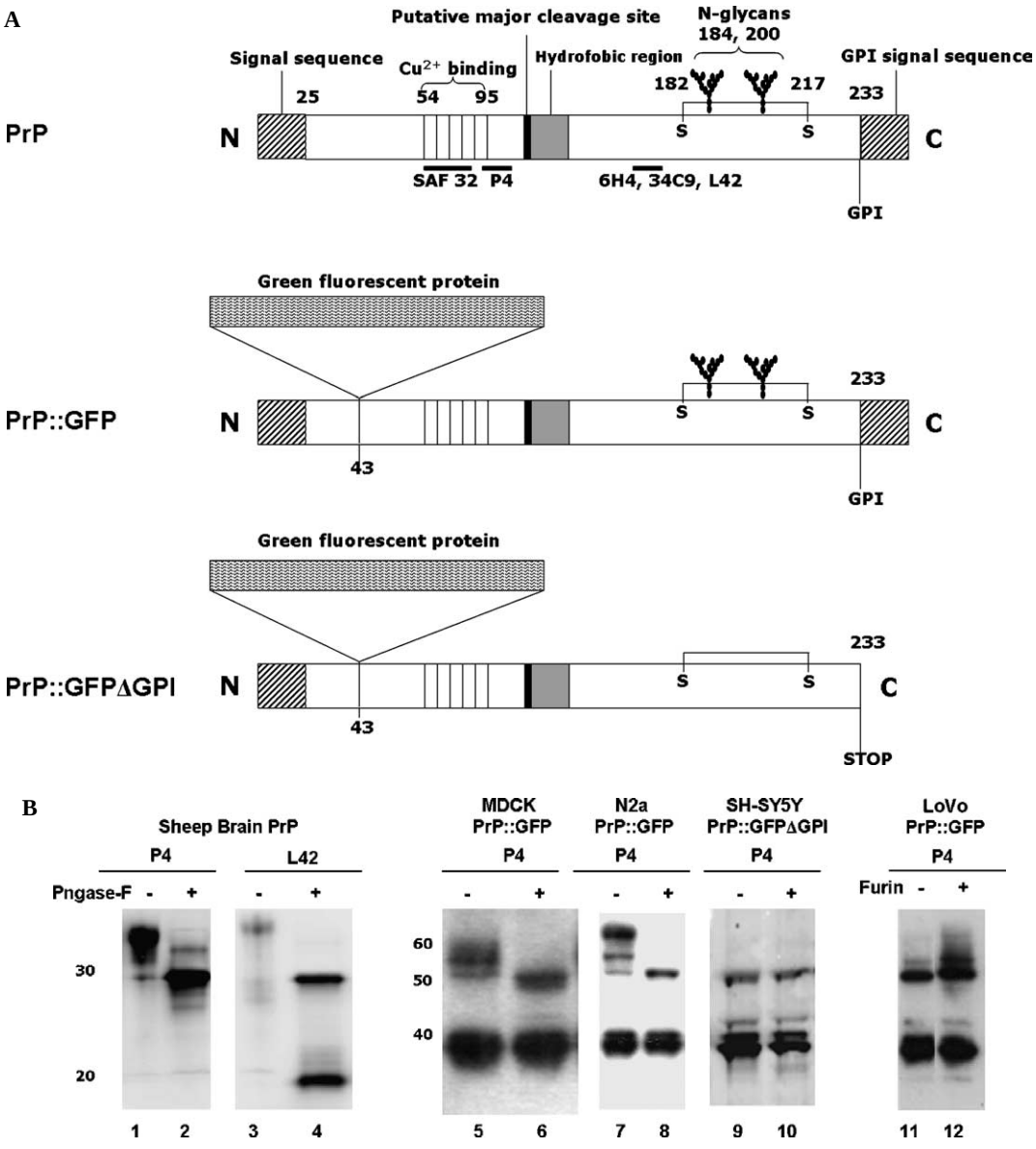

Fig. 1. Ovine PrP and PrP::GFP constructs. (A) Features and binding sites of antibodies on both sides of the putative major cleavage site. (B) Patterns of PrP cleavage in sheep brain (lanes 1–4) and different cell lines transfected with PrP::GFP (lanes 5–8, and 11 and 12) and PrP::GFPΔGPI (lanes 9 and 10). Samples from sheep brain and cell lysates were treated with Pngase-F as indicated. The absence or presence of furin in the LoVo cells is indicated in lanes 11 and 12.

similarly processed in all four cell lines used in this study. The proteolytic processing of PrP::GFP appears unrelated to the proteinase furin as the furin-deficient LoVo cell line processed PrP::GFP with the same efficiency as LoVo cells stably transfected with furin (Fig. 1B, lanes 11 and 12). Analysis of the proteolytic maturation of PrP constructs devoid of GPI anchor (PrP::GFPΔGPI) revealed that their processing is indistinguishable from GPI-anchored PrPs (Fig. 1B, lanes 9 and 10). Notably, PrP::GFPΔGPI proteins were unglycosylated.

To explore the effect of primary structure on the proteolytic processing of PrP, we have performed a number of substitutions of amino-acids affecting the putative cleavage site (Figs. 2A and B). Analyses of clones carrying these substitutions reveal that the pattern and apparent efficiency of PrP processing are unaffected by the mutations, even after replacing amino-acids KHV (113–115) with three alanines (Fig. 2C, lanes 9 and 10).

In order to utilise the 3F4 antibody in our studies of the processing of PrP, we generated an ovine PrP::GFP construct carrying the 3F4 epitope by substituting V115M (Figs. 2A and B). As shown in Fig. 2C, lanes 11 and 12, the processing of PrP::GFP V115M, as revealed by the P4 antibody, is unaffected by the mutation. However, when probed with the 3F4 antibody it is clearly illustrated that this epitope is severely affected by the processing event, as immunoreactivity is largely confined to full-length molecules (Fig. 2C, lanes 13 and 14).

MDCK cells and the other cell lines were exposed to various proteinase inhibitors in attempts to inhibit the

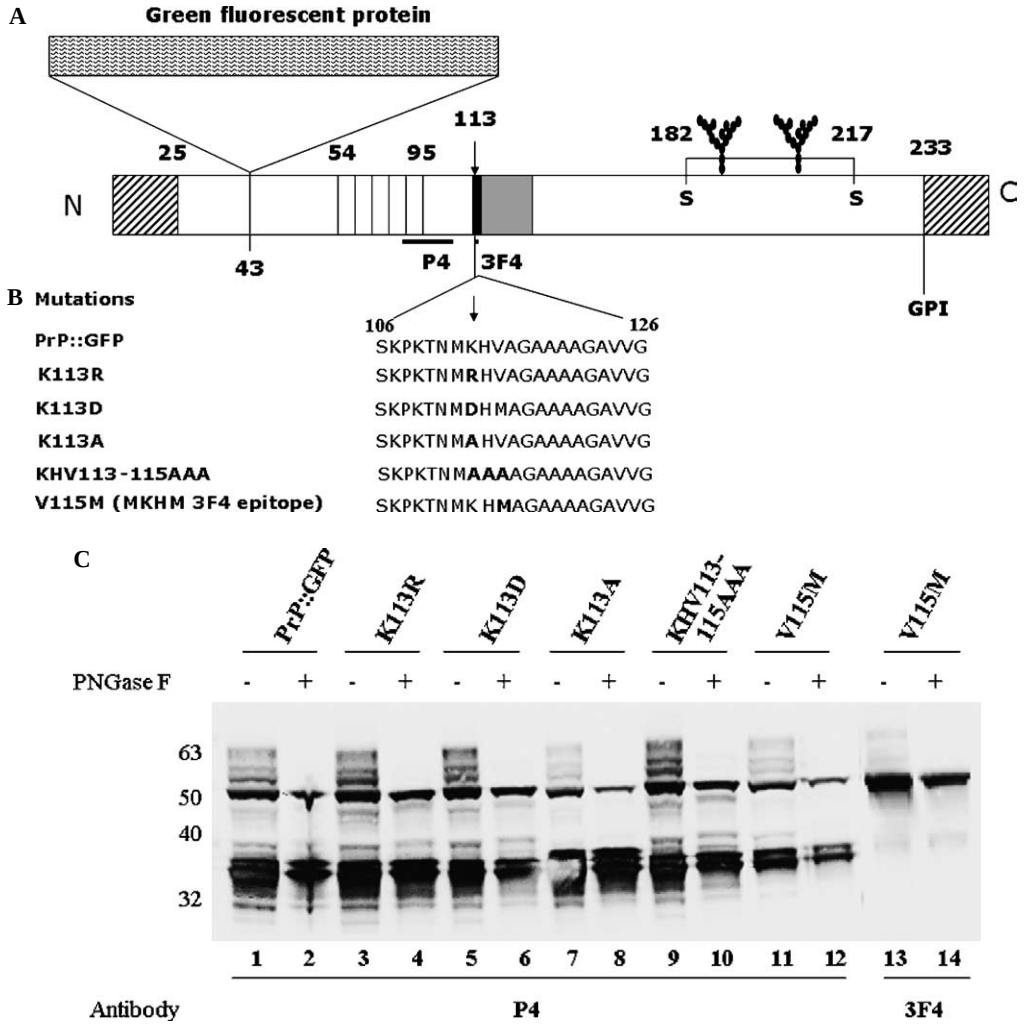

Fig. 2. Site-directed mutagenesis. (A) Schematic organisation of PrP::GFP, highlighting the major cleavage site (arrow) and binding sites for the monoclonal antibodies 3F4 and P4. (B) Mutations introduced in the PrP::GFP construct at the putative cleavage site of PrP are given in bold letters. The insertion of the 3F4 epitope (V115M) is indicated. (C) Western blot analysis of N2a cells transiently transfected with mutated PrP::GFP, analysed with the P4 (lanes 1–12) or 3F4 (lanes 13 and 14) antibodies.

Table 2
Estimated and observed molecular masses of PrP and PrP::GFP fusion proteins and fragments

PrP fragment	Estimated molecular mass in kDa[a]				Molecular mass in SDS electrophoresis		
Amino acids	Peptide mass	*N*-glycan	*N*-glycan	GPI anchor	Without PNGase F	With PNGase F	PrP::GFP chimaera
25–233	22.7	4.5	4.5	4.5	27–37	27.2	52–63
113–233	13.9	4.5	4.5	4.5	25–27[b]	18.4	25–27
25–112	8.9	—	—	—	8.9	8.9	35.9

[a] Peptide masses were calculated by use of the computer program Vector-NTI (Informax, USA). Masses given for *N*-glycans and GPI anchor are estimates based upon molecular masses observed in SDS electrophoresis in this paper and elsewhere, e.g., full-length deglycosylated PrP with its GPI anchor intact runs at about 27.2 kDa in SDS electrophoresis.

[b] The presence of this C-terminal fragment is often obscured by less glycosylated full-length PrP molecules when analysed with intact *N*-glycans, C-terminal fragments are, however, easily visualized after treatment with PNGase-F, as illustrated in Fig. 1B, lanes 3 and 4. The molecular masses of full-length and cleaved PrP::GFP fusion proteins analysed in this paper are also given. The molecular mass of GFP is approximately 27 kDa.

proteolytic processing of PrP::GFP as shown in Figs. 3A and B. We did not observe any significant reduction in the processing activity after inhibition of lysosomal proteinases by increasing concentrations of leupeptin (Fig. 3A, lanes 2–5) and zinc-metalloproteinases by use of galardin (Fig. 3A, lanes 6 and 7). Notably, concentrations of galardin reaching 100 μM were tested without any apparent effect on the processing of PrP::GFP (not shown). As shown in Fig. 3B, treatment with NH_4Cl (lane 2) and aprotinin (lane 3) for 16 h failed to affect the processing

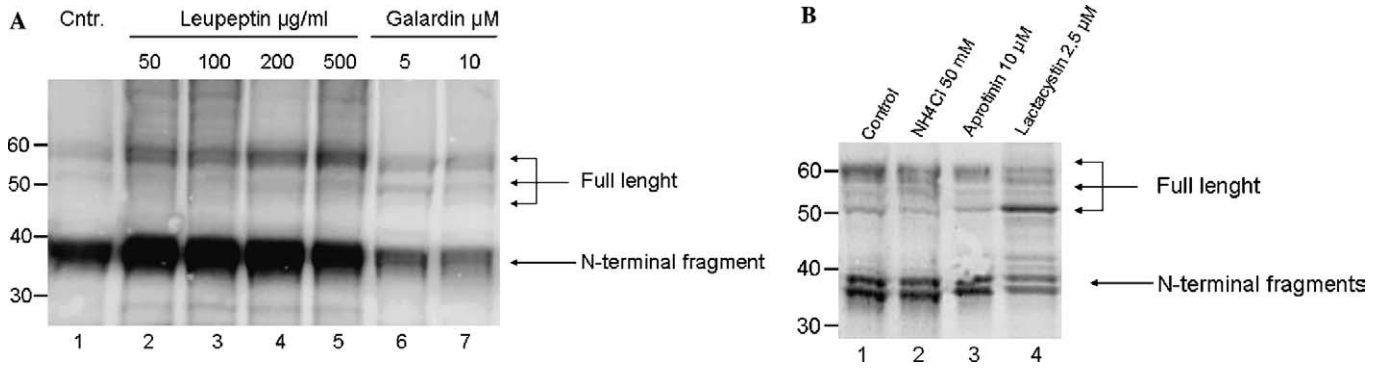

Fig. 3. Attempts to inhibit the constitutive cleavage of PrP::GFP in stably transfected (A) MDCK II and (B) N2a cells by use of different classes of proteinase inhibitors. (A) Cells were untreated (lane 1) or treated overnight (16 h) with leupeptin (lanes 2–5) and galardin (lanes 6 and 7) as indicated. (B) Cells were untreated (lane 1) or treated overnight with NH_4Cl (lane 2) or aprotinin (lane 3) and the proteasome inhibitor lactacystin (lane 4).

of PrP::GFP, while incubation with the irreversible proteasome inhibitor lactacystin (lane 4) led to an increase in unglycosylated full-length PrP::GFP.

As illustrated in Figs. 4A–C, treatment with Baf A_1 for 16 h allowed more unprocessed PrP to be recovered, especially in the apical medium of MDCK. The average increase of unprocessed PrP, relative to total PrP, based on three separate experiments, was from about 16% in the controls to over 30% after Baf A_1 treatment (Fig. 4B). The larger part of this increase in PrP immunoreactivity was recovered in the apical medium of MDCK cells, as highlighted in Fig. 4C. These experiments also provide some information

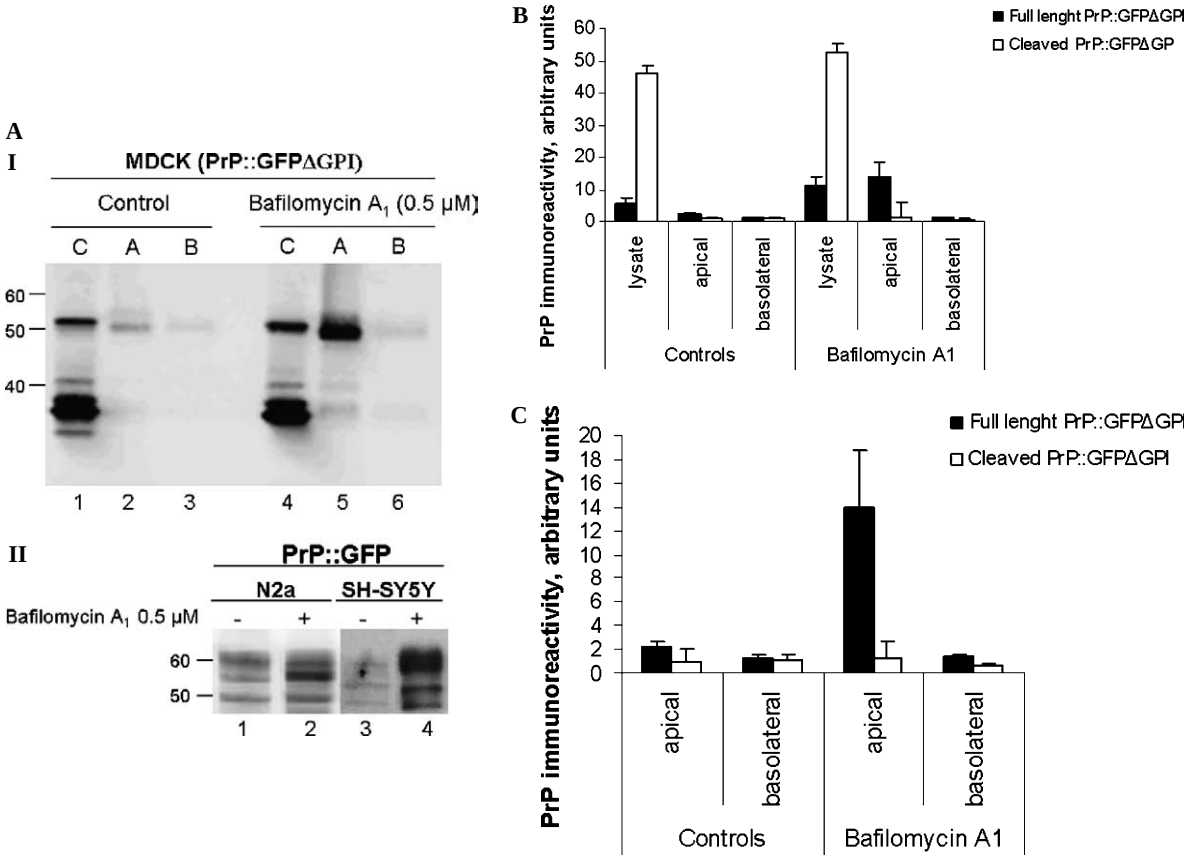

Fig. 4. Baf A_1 increases the amount of full-length PrP. (A, panel I) shows Western blot of cell lysate (C), apical (A), and basolateral (B) media of MDCK II cells stably transfected with PrP::GFPΔGPI. Cells were grown on filters and left untreated (control) or treated with Baf A_1 (0.5 µM) for 16 h. Panel II shows the effect on full-length PrP::GFP molecules of incubation for 16 h with 0.5 µM Baf A_1 in N2a and SH-SY5Y cells expressing PrP::GFP. (B) Quantitative analysis of full-length and cleaved PrP::GFPΔGPI in cell lysates and cell media of control versus Baf A_1-treated MDCK II cells. Data are given as means ± SEM of three independent experiments. PrP immunoreactivity is given in arbitrary units. (C) The same data as shown in (B), but omitting the cell lysates to highlight the increased amount of full-length PrP::GFPΔGPI in apical but not basolateral media after treatment with Baf A_1.

concerning the sorting of this PrP::GFP protein in MDCK cells and how Baf A_1 exerts an effect on this sorting. In the absence of Baf A_1 the secretion of PrP::GFPΔGPI into the apical and basolateral media is about 2:1, respectively (Fig. 4A, panel I, lanes 2 and 3), while in the presence of Baf A_1, secretion of PrP::GFPΔGPI is greatly increased and more stringently secreted into the apical medium (lane 5), with no increase in the basolateral medium (lane 6). The increase in full-length PrP::GFP expressed in N2a and SH-SY5Y cells after treatment with Baf A_1 for 16 h is given in Fig. 4A, panel II, lanes 1–4.

Discussion

Although the proteolytic processing of PrP was observed in the early 1990s, it is still relatively poorly understood. Notably, the fact that the epitope for the 3F4 monoclonal antibody, the most commonly used antibody in prion research, is destroyed by the proteolytic processing of PrP may have led to a somewhat simplified view of the cellular biology of PrP [7]. This point is also clearly illustrated in the PrP::GFP model we have employed. Analysis of brain or cell culture derived PrP from different species, including birds, has shown that a considerable fraction of the total PrP pool has undergone proteolytic processing [2,3,7]. To what extent truncated PrPs can contribute to the de novo generation of malformed PrP^{Sc} is presently unknown [7], but an interaction between PrP^{C} and PrP^{Sc} resulting in disturbances of the normal processing of PrP^{C} cannot be ruled out. The cleavage of PrP shares a number of features with proteins that are cleaved in the vicinity of a transmembrane segment, known as juxtamembrane cleavage. Detailed epitope mapping, comparison of size, and glycosylation patterns of the cleavage products of the PrP::GFP constructs used in this study clearly show that they were processed similarly if not identical to wt-PrP. This model is further strengthened by the extreme affinity of the monoclonal antibody P4 towards ovine PrP in Western blots. The P4 antibody was raised against a synthetic peptide covering amino-acids 89–104 in the ovine PrP [21]. It thus binds to the N-terminal fragment produced by the major cleavage around amino-acid 113.

We find that only a limited amount of N-terminal cleavage products are released into the cell culture medium; rather, these are retained within the cells. If the cleavage of PrP::GFP took place at the cell surface or during recycling, one would have to expect the bulk of N-terminal fragments to be released to the culture medium during this process. Retention of N-terminal fragments within cells is, however, in agreement with a recent report in which a double-labelled fluorescent mouse PrP was studied in N2a cells, where N-terminal fragments were retained within the cells, possibly in vesicular structures in association with cytoskeleton components [22]. Another feature of the model employed in this study is that if a cleavage of PrP some 10–20 amino-acids closer to the N-terminus should occur at a significant frequency [7], this would be expected to directly affect the P4 epitope. Our data do not support such a notion because in our system N-terminal cleavage products are detected similarly with MAb SAF32, which binds in the octa-repeat region, and P4. This appears to rule out an alternative cleavage of PrP affecting the region covering amino-acids 80–90 as N-terminal fragments thus derived cannot be detected by P4. However, if a cleavage occurred around amino-acid 105 in the ovine PrP, just C-terminal to the P4 epitope, corresponding to K101 in the human sequence, the P4 epitope would be intact in the N-terminal fragment. We have explored this by substituting V115 with M115 in the ovine PrP, thus establishing the 3F4 epitope, reasoning that if a separate cleavage took place around amino-acid 105, the 3F4 epitope would be intact on the C-terminal fragment since this epitope probably spans amino-acids 107–115 according to ovine PrP [23]. We have, however, failed to detect such a C-terminal fragment. Thus, the exact difference in structure between the two N-terminal fragments, routinely observed with our model, as seen in Fig. 3B, remains to be determined. Our studies of 3F4 tagged ovine PrP::GFP, however support evidence from other species showing that this epitope is destroyed as a result of the proteolytic processing of PrP. This also underlines the similarity of the processing of PrP::GFP as studied here and the previously reported processing of brain PrP in humans [5]. However, we do detect some slightly heavier N-terminal fragments also with 3F4, suggesting that a minor portion of the PrP molecules are cleaved just C-terminal to amino-acid 115, leaving the 3F4 epitope intact on the N-terminal fragment, indicating a relatively low specificity for the cleavage.

In order to analyse this further and possibly to inhibit the cleavage, we inserted a number of amino-acid substitutions affecting the putative cleavage site. None of these mutations affected the processing of PrP::GFP, which suggests that the enzyme(s) performing this cleavage operates largely independent of the primary structure at the cleavage site. Thus, it seems likely that other structural domains of PrP are recognised by the processing enzyme(s). Data from cells transfected with PrP lacking its GPI anchor (PrP::GFPΔGPI) effectively show that the structural features that guide the processing activity are neither *N*-glycan modifications nor the GPI anchor itself. Furthermore, efficient cleavage of PrP::GFPΔGPI indicates that GPI-directed raft association of PrP is not a prerequisite for proteolytic processing, which would probably be expected to be the case if the cleavage occurred during endocytic recycling of PrP or by a raft-associated proteolytic activity.

Our attempts to inhibit the processing of PrP::GFP by means of chemicals were also largely negative, except for Baf A_1 which resulted in a strong increase in recovery in full-length forms of PrP. An increase in full-length unglycosylated forms of PrP was, however, seen also after treatment with the irreversible proteasome inhibitor lactasystin (Fig. 3B, lane 4). This finding, which is in accordance with a comprehensive study of the role of proteasomes in the turnover of wild-type and mutated PrPs [24], most likely

reflects that even in cell cultures expressing low to moderate levels of transgenic PrP, as used in this study, a certain fraction of the newly synthesised proteins will be subjected to proteasomal degradation. The effects exerted by Baf A_1 are interesting in view of the inhibitory effect that Baf A_1 has on BACE-1 which is a membrane-bound aspartyl proteinase resident in the endoplasmic reticulum and Golgi, particularly active in the trans-Golgi network (TGN) [19,25]. Interestingly, Baf A_1 appears not to inhibit α-secretase activities [19]. Since BACE 1 and a large number of other proteinases are synthesised as zymogens that must be proteolytically activated by convertases, such as furin (reviewed by [26]), which is resident in TGN, we analysed the proteolytic processing of PrP::GFP in the furin-deficient human colon cancer cell line LoVo. We could observe no difference in PrP::GFP processing between cells with or without furin. It thus appears that the cleavage of PrP::GFP as observed in our system is not furin dependent. Notably, other enzymes in the pro-protein convertase family, such as PC7, has been shown to be active and able to activate both TACE and ADAM 10 in the absence of furin in LoVo cells [27,28]. Therefore, a role for TACE and ADAM 10 in the processing of PrP cannot be excluded.

Baf A_1 specifically inhibits the V-H^+/ATPase which is localised to compartments of the endocytic and secretory pathways, and is the major acidification mediator of the lumen of these organelle systems. It is interesting to note that neutralisation with NH_4Cl failed to mimic the effects seen with Baf A_1. The lack of inhibition of PrP processing of other inhibitors of lysosomal proteinases, such as leupeptin and aprotinin, strongly suggests that the processing is non-lysosomal and that the effects seen with Baf A1 probably stems from effects exerted on other acidified vesicles or organelles. Further, the lack of inhibitory effect even of very large concentrations of the broad spectrum metalloproteinase inhibitor galardin shows that this processing, if metalloproteinase dependent, is probably not occurring at the plasma membrane or endocytic compartments accessible to the inhibitor. This, however, does not necessarily contradict previous observations pointing to a role for zinc-metalloproteinases in the processing of PrP [13], because complete inhibition of such activities is notoriously difficult to achieve. Furthermore, the phorbol ester-stimulated shedding of full-length PrP which has been ascribed to an α-secretase like activity [14] has not been studied here.

The predominant apical secretion of PrP::GFPΔGPI in stably transfected MDCK cells observed here, particularly after treatment with Baf A1 (approximately 90% apically), deserves attention, since neutralisation of the lumen of acidic organelles is known to increase the apical secretion stringency [29,30]. A similar medium distribution was observed with GPI-anchored PrP::GFP (not shown). Although we did not differentiate with respect to cellular sub-localisation of the PrP::GFP fusion protein variants, our observations might complement the current view of polarised transport of PrP in epithelial MDCK cells. A predominant basolateral localisation of PrP has previously been reported [31], but in that case, neither cellular localisation of cleaved PrP nor the appearance of PrP in the media was studied. However, it has recently been shown that the hydrophobic domain of PrP can function as a dominant signal for basolateral sorting of PrP in MDCK cells [32]. Interestingly, this domain is not altered in any of the PrP constructs utilised in this study and would thus be expected to direct the sorting of PrP::GFP proteins to the basolateral membrane or medium. This, however, seems not to be the case.

Further studies are needed to get the total picture of PrP sorting and transport in MDCK cells.

In summary, the data presented here indicate that a considerable sub-population of PrP molecules is proteolytically cleaved in an amazingly robust process, possibly during passage through the secretory pathway, by one or more enzymes of which some may have patterns of inhibition similar to that of BACE 1. This PrP processing is independent of furin and apparently of the primary sequence at the cleavage site. The precise cellular compartment for the processing or whether trapping of PrP in transmembrane conformations is involved in the processing remains to be elucidated.

Acknowledgments

We thank David Griffiths for proofreading of the manuscript and Berit Christophersen and Rosa Ferreira for excellent technical assistance. We greatly thank Jörg Tatzelt for providing us the SH-SY5Y and N2a cell lines. This work was supported by grants from the Norwegian Research Council.

References

[1] C. Weissmann, The state of the prion, Nat. Rev. Microbiol. 2 (2004) 861–871.
[2] K.M. Pan, N. Stahl, S.B. Prusiner, Purification and properties of the cellular prion protein from Syrian hamster brain, Protein Sci. 1 (1992) 1343–1352.
[3] D.A. Harris, M.T. Huber, P. van Dijken, S.L. Shyng, B.T. Chait, R. Wang, Processing of a cellular prion protein: identification of N- and C-terminal cleavage sites, Biochemistry 32 (1993) 1009–1016.
[4] S.L. Shyng, M.T. Huber, D.A. Harris, A prion protein cycles between the cell surface and an endocytic compartment in cultured neuroblastoma cells, J. Biol. Chem. 268 (1993) 15922–15928.
[5] S.G. Chen, D.B. Teplow, P. Parchi, J.K. Teller, P. Gambetti, L. Autilio-Gambetti, Truncated forms of the human prion protein in normal brain and in prion diseases, J. Biol. Chem. 270 (1995) 19173–19180.
[6] A. Mange, F. Beranger, K. Peoc'h, T. Onodera, Y. Frobert, S. Lehmann, Alpha- and beta-cleavages of the amino-terminus of the cellular prion protein, Biol. Cell 96 (2004) 125–132.
[7] T. Pan, R. Li, B.S. Wong, T. Liu, P. Gambetti, M.S. Sy, Heterogeneity of normal prion protein in two- dimensional immunoblot: presence of various glycosylated and truncated forms, J. Neurochem. 81 (2002) 1092–1101.
[8] R.J. Kascsak, R. Rubenstein, P.A. Merz, M. Tonna-DeMasi, R. Fersko, R.I. Carp, H.M. Wisniewski, H. Diringer, Mouse polyclonal and monoclonal antibody to scrapie-associated fibril proteins, J. Virol. 61 (1987) 3688–3693.
[9] A. Taraboulos, M. Scott, A. Semenov, D. Avrahami, L. Laszlo, S.B. Prusiner, Cholesterol depletion and modification of COOH-terminal

targeting sequence of the prion protein inhibit formation of the scrapie isoform, J. Cell Biol. 129 (1995) 121–132.
[10] J.A. Kornblatt, S. Marchal, H. Rezaei, M.J. Kornblatt, C. Balny, R. Lange, M.P. Debey, G. Hui Bon Hoa, M.C. Marden, J. Grosclaude, The fate of the prion protein in the prion/plasminogen complex, Biochem. Biophys. Res. Commun. 305 (2003) 518–522.
[11] M. Praus, G. Kettelgerdes, M. Baier, H.G. Holzhutter, P.R. Jungblut, M. Maissen, G. Epple, W.D. Schleuning, E. Kottgen, A. Aguzzi, R. Gessner, Stimulation of plasminogen activation by recombinant cellular prion protein is conserved in the NH2-terminal fragment PrP23-110, Thromb. Haemost. 89 (2003) 812–819.
[12] A. Jimenez-Huete, P.M. Lievens, R. Vidal, P. Piccardo, B. Ghetti, F. Tagliavini, B. Frangione, F. Prelli, Endogenous proteolytic cleavage of normal and disease-associated isoforms of the human prion protein in neural and non-neural tissues, Am. J. Pathol. 153 (1998) 1561–1572.
[13] B. Vincent, E. Paitel, P. Saftig, Y. Frobert, D. Hartmann, B. De Strooper, J. Grassi, E. Lopez-Perez, F. Checler, The disintegrins ADAM10 and TACE contribute to the constitutive and phorbol ester-regulated normal cleavage of the cellular prion protein, J. Biol. Chem. 276 (2001) 37743–37746.
[14] E.T. Parkin, N.T. Watt, A.J. Turner, N.M. Hooper, Dual mechanisms for shedding of the cellular prion protein, J. Biol. Chem. 279 (2004) 11170–11178.
[15] K.S. Lee, A.C. Magalhaes, S.M. Zanata, R.R. Brentani, V.R. Martins, M.A. Prado, Internalization of mammalian fluorescent cellular prion protein and N-terminal deletion mutants in living cells, J. Neurochem. 79 (2001) 79–87.
[16] L. Ivanova, S. Barmada, T. Kummer, D.A. Harris, Mutant prion proteins are partially retained in the endoplasmic reticulum, J. Biol. Chem. 276 (2001) 42409–42421.
[17] A. Negro, C. Ballarin, A. Bertoli, M.L. Massimino, M.C. Sorgato, The metabolism and imaging in live cells of the bovine prion protein in its native form or carrying single amino acid substitutions, Mol. Cell. Neurosci. 17 (2001) 521–538.
[18] H. Lorenz, O. Windl, H.A. Kretzschmar, Cellular phenotyping of secretory and nuclear prion proteins associated with inherited prion diseases, J. Biol. Chem. 277 (2002) 8508–8516.
[19] J. Knops, S. Suomensaari, M. Lee, L. McConlogue, P. Seubert, S. Sinha, Cell-type and amyloid precursor protein-type specific inhibition of A beta release by bafilomycin A1, a selective inhibitor of vacuolar ATPases, J. Biol. Chem. 270 (1995) 2419–2422.
[20] J. Safar, W. Wang, M.P. Padgett, M. Ceroni, P. Piccardo, D. Zopf, D.C. Gajdusek, C.J. Gibbs Jr., Molecular mass, biochemical composition, and physicochemical behavior of the infectious form of the scrapie precursor protein monomer, Proc. Natl. Acad. Sci. USA 87 (1990) 6373–6377.
[21] S. Harmeyer, E. Pfaff, M.H. Groschup, Synthetic peptide vaccines yield monoclonal antibodies to cellular and pathological prion proteins of ruminants, J. Gen. Virol. 79 (1998) 937–945.
[22] N.S. Hachiya, K. Watanabe, Y. Sakasegawa, K. Kaneko, Microtubules-associated intracellular localization of the NH_2-terminal cellular prion protein fragment, Biochem. Biophys. Res. Commun. 313 (2004) 818–823.
[23] D.C. Bolton, S.J. Seligman, G. Bablanian, D. Windsor, L.J. Scala, K.S. Kim, C.M. Chen, R.J. Kascsak, P.E. Bendheim, Molecular location of a species-specific epitope on the hamster scrapie agent protein, J. Virol. 65 (1991) 3667–3675.
[24] B. Drisaldi, R.S. Stewart, C. Adles, L.R. Stewart, E. Quaglio, E. Biasini, L. Fioriti, R. Chiesa, D.A. Harris, Mutant PrP is delayed in its exit from the endoplasmic reticulum, but neither wild-type nor mutant PrP undergoes retrotranslocation prior to proteasomal degradation, J. Biol. Chem. 278 (2003) 21732–21743.
[25] M. Khvotchev, T.C. Sudhof, Proteolytic processing of amyloid-beta precursor protein by secretases does not require cell surface transport, J. Biol. Chem. 279 (2004) 47101–47108.
[26] K. Nakayama, Furin: a mammalian subtilisin/Kex2p-like endoprotease involved in processing of a wide variety of precursor proteins, Biochem. J. 327 (1997) 625–635.
[27] K. Endres, A. Anders, E. Kojro, S. Gilbert, F. Fahrenholz, R. Postina, Tumor necrosis factor-alpha converting enzyme is processed by proprotein-convertases to its mature form which is degraded upon phorbol ester stimulation, Eur. J. Biochem. 270 (2003) 2386–2393.
[28] A. Anders, S. Gilbert, W. Garten, R. Postina, F. Fahrenholz, Regulation of the alpha-secretase ADAM10 by its prodomain and proprotein convertases, FASEB J. 15 (2001) 1837–1839.
[29] M.J. Caplan, J.L. Stow, A.P. Newman, J. Madri, H.C. Anderson, M.G. Farquhar, G.E. Palade, J.D. Jamieson, Dependence on pH of polarized sorting of secreted proteins, Nature 329 (1987) 632–635.
[30] K. Parczyk, C. Kondor-Koch, The influence of pH on the vesicular traffic to the surface of the polarized epithelial cell, MDCK, Eur. J. Cell Biol. 48 (1989) 353–359.
[31] D. Sarnataro, S. Paladino, V. Campana, J. Grassi, L. Nitsch, C. Zurzolo, PrP^C is sorted to the basolateral membrane of epithelial cells independently of its association with rafts, Traffic 3 (2002) 810–821.
[32] A. Uelhoff, J. Tatzelt, A. Aguzzi, K.F. Winklhofer, C. Haass, A pathogenic PrP mutation and doppel interfere with polarized sorting of the prion protein, J. Biol. Chem. 280 (2005) 5137–5140.